Abundance Distribution in Supernova Remnant Cas A

Yasuhide MATSUO[1], Masa-aki HASHIMOTO[1] and Kenzo ARAI[2]

[1]*Department of Physics, Kyushu University, Fukuoka 810-8560*
[2]*Department of Physics, Kumamoto University, Kumamoto 860-8555*

(Received September 30, 2010)

Two dimensional hydrodynamical simulations of supernova remnant Cas A are performed starting from the onset of explosion to the present phase. Before the explosion, distributions of circumstellar medium is constructed, where the medium is assumed to be ejected from a progenitor. A supernova simulation is carried out by two dimensional hydrodynamical calculation. It is found that the Rayleigh-Taylor instability is advanced from the boundary between hydrogen and helium layers. The instability from silicon and iron layers is not grown enough to induce the observed mixing of materials. It is suggested that mixing before the explosion and/or instability at the boundary of silicon and iron layers due to different distributions of circumstellar medium is needed to explain the observations.

§1. Introduction

It is Cassiopeia A (Cas A) that is the youngest supernova remnant in our Galaxy. Cas A is the brightest radio source so far.[1)] Moreover, it has been observed in possible bands of the spectrum: radio,[2)] infrared,[3)] visible[4)] and X-ray.[5)] The yields of hydrodynamical simulations are compared in detail with the observed properties. Therefore, Cas A becomes one of the main targets for numerical simulations of supernova explosion.

The observations of X-ray from Cas A indicate[6)] that the progenitor exploded in A.D. 1671. The distance to Cas A is determined to be 3.4 kpc[7)] and its size is $2-3$ pc. Although the type of the supernova for Cas A was inferred to be Ib/c,[8)] it has been finally identified to be type IIb from the observation of light echo,[9)] which indicates the explosion of a helium star.

Recent observations have clearly shown there exist a peculiar regions where irons distribute outside the Si-rich layer.[10)] Since this observational evidence cannot be explained in terms of a spherical explosion model, some kinds of mixing between Si- and Fe-rich layers should occur in large scale. Although there are no detailed investigations about the mixing of Cas A, we can infer the mechanism of the mixing processes: the Rayleigh-Taylor instabilities inside the star,[11)] interactions between the supernova shock and the circumstellar medium[12)] and the non-spherical explosion such as jets and/or standing accretion shock instability.[13)]

In the present paper, we investigate possible mixing between Si- and Fe-layers due to the Rayleigh-Taylor instability during supernova explosion, using a presupernova model with circumstestellar medium ejected from a progenitor. Two dimensional hydrodynamical simulations are performed to the present remnant phase of Cas A by extending the technical method used for the mixing of supernova 1987A.[11),14)]

§2. Basic equations

Let D/Dt be the Lagrange differentiation, which varies along the fluid particle. The non-relativistic equations of fluid dynamics relevant for the simulations are

$$\frac{D\rho}{Dt} = -\rho\nabla\cdot\boldsymbol{v}, \tag{2.1}$$

$$\rho\frac{D\boldsymbol{v}}{Dt} = -\nabla P - \rho\nabla\left(\Phi - \frac{GM_{\rm pt}}{r}\right), \tag{2.2}$$

$$\rho\frac{D}{Dt}\left(\frac{e}{\rho}\right) = -P\nabla\cdot\boldsymbol{v}, \tag{2.3}$$

where ρ, P, e and $\boldsymbol{v}$ are the density, pressure, internal energy density and velocity, respectively, of fluid. $M_{\rm pt}$ is the mass of the point source at the center. Self gravitational potential Φ is obtained by solving the following Poisson equation

$$\nabla^2\Phi = 4\pi G\rho. \tag{2.4}$$

We define the radius $R_{\rm ph}$ of the photosphere to be

$$\int_{R_{\rm ph}}^{\infty}\rho(r)\kappa_{\rm es}dr = \frac{2}{3},$$

where $\kappa_{\rm es}$ is the opacity due to the electron scattering: $\kappa_{\rm es} = 0.20(1+X)\,{\rm cm}^2\,{\rm g}^{-1}$ with the hydrogen mass fraction X.

To solve the above set of equations (2.1)–(2.4), we need an equation of state. Inside the photosphere, $r \le R_{\rm ph}$, we take radiation and gases composed of electrons and ions:

$$P = P_{\rm rad} + P_{\rm gas},$$
$$e = 3P_{\rm rad} + \frac{3}{2}P_{\rm gas},$$

with

$$P_{\rm rad} = \frac{1}{3}aT^4,$$
$$P_{\rm gas} = \frac{R}{\mu},\rho T$$

where T is the temperature, a is the radiation constant, R is the gas constant and μ is the mean molecular weight.

Outside $R_{\rm ph}$ radiation becomes free, so we set

$$P = P_{\rm gas},$$
$$e = \frac{3}{2}P_{\rm gas}.$$

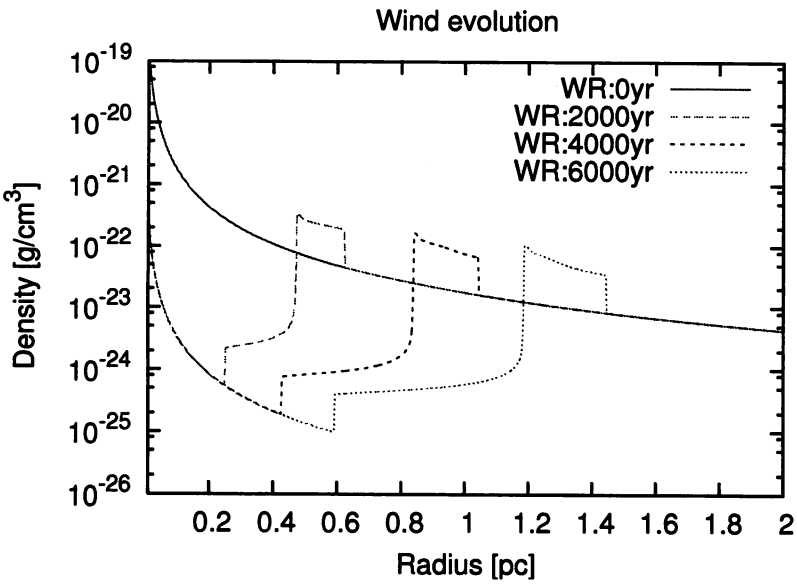

Fig. 1. Evolution of WR and RSG winds. The wind shells are formed around the boundary between the two winds.

For a high temperature region above 5×10^9 K, all materials are in nuclear statistical equilibrium. When $T \leq 5 \times 10^9$ K, we take into account 14 species of nuclei: p, ^{4}He, ^{12}C, ^{16}O, ^{20}Ne, ^{24}Mg, ^{28}Si , ^{32}S, ^{36}Ar, ^{40}Ca, ^{44}Ti, ^{48}Cr, ^{52}Fe and ^{56}Ni. The abundance flow (advection) can be followed by solving (2.1) for individual elements k with the mass fraction X_k, where $X_k = \rho_k/\rho$.

Once ρ and T are determined, then the nuclear reaction rates are evaluated. Consequently, the generated nuclear energies are added to the internal energy.

§3. Initial Models

3.1. *Construction of the circumstellar medium*

Observations indicate that a progenitor of Cas A had lost most hydrogen-rich envelope before the explosion.[9] We may infer that the progenitor was a Wolf-Rayet (WR) star: the progenitor experiences three stellar evolutionary stages from the main sequence (MS) stage via the red super giant (RSG) stage finally to the WR stage.

According to the calculation of stellar evolution,[12] the RSG stage continues over 0.6 Myr with a typical wind velocity 10 km s^{-1}. The boundary between the MS and RSG winds locates at about 6 pc, which is much further compared to the forward shock front of 2.5 pc.[15] Therefore, we neglect the effects of the MS wind to the evolution of stellar wind.

If we assume the RSG wind is spherical and steady,[16] then density in the wind

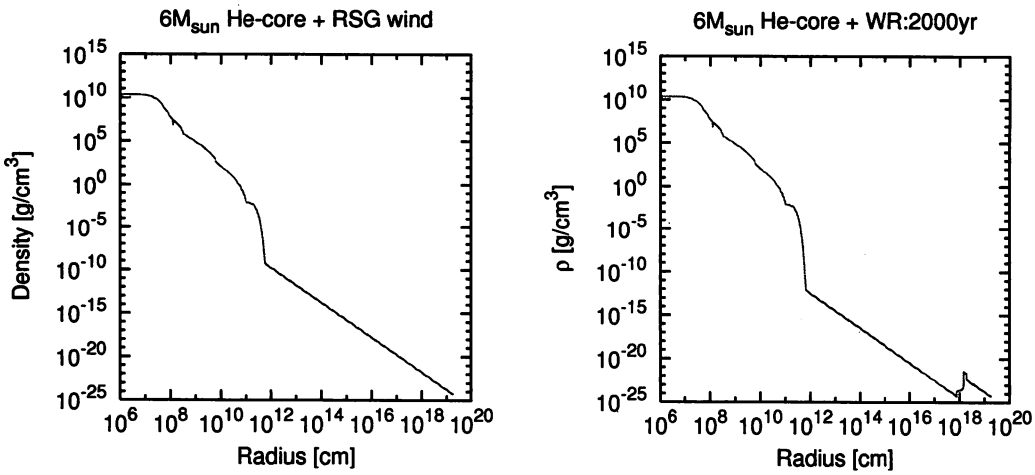

Fig. 2. Density distribution of the initial models for $T_{\rm WR} = 0$ (left panel) and 2000 yr (right panel). The original presupernova core of $6M_\odot$ lies inside 10^{11} cm. The knob around 10^{18} cm in the right panel corresponds to the WR+RSG shell.

is written from (2.1) as

$$\rho(r) = \frac{\dot{M}_{\rm RSG}}{4\pi r^2 v_{\rm RSG}}, \tag{3.1}$$

where $\dot{M}_{\rm RSG}$ is the mass loss rate and $v_{\rm RSG}$ is the velocity of the RSG wind. From the stellar evolution calculations,[17] we take $\dot{M}_{\rm RSG} = 1.54 \times 10^{-5}\, M_\odot {\rm yr}^{-1}$, $v_{\rm RSG} = 4.7$ km s^{-1} and $T_{\rm RSG} = 10^3$ K. Under the above condition of the RSG wind, the WR winds are advected[18] with $\dot{M}_{\rm WR} = 9.6 \times 10^{-6}\, M_\odot {\rm yr}^{-1}$, $v_{\rm WR} = 1.7 \times 10^3$ km s^{-1} and $T_{\rm WR} = 10^4$ K.

We calculate the spherical stellar wind from 0.01 to 2 pc with the 2000 equally stretched meshes. The evolution of the winds is shown in Fig. 1. Since the WR wind becomes three orders in magnitude faster than the RSG wind, the WR wind pushes the back of the RSG wind. Consequntly, high density shells (WR+RSG shells) are formed around the boundary between the two winds.

It has been reported[19] that the duration $t_{\rm WR}$ of the WR stage could be less than about 3500 yr. Taking into account the uncertainty in $t_{\rm WR}$, we consider two cases $t_{\rm WR} = 0$ and 2000 yr.

3.2. *Observational constraints due to one dimensional simulations*

We adopt the presupernova model of a $6M_\odot$ He-core.[20] Initial models are constructed by connecting this presupernova model with the WR and RSG winds described in the last subsection. Figure 2 shows the density distribution of the initial models. The left panel indicates the case $t_{\rm WR} = 0$ and the right one is the case $t_{\rm WR} = 2000$ yr. Note that there appears a knob around 10^{18} cm, which corresponds to the WR + RSG shell.

Table I gives the positions $R_{\rm fs}$ of the forward shock and $R_{\rm rs}$ of the reverse shock for models with the input energy of explosion $E_{\rm in} = 2 - 4 \times 10^{51}$ erg in two cases.

Table I. Models associated to stellar winds. $t_{\rm WR}$ is the duration of the WR stage, $E_{\rm in}$ is the input energy of explosion, $R_{\rm fs}$ and $R_{\rm rs}$ are the locations of the forward and reverse shocks, respectively.

Models	WR0E2	WR0E3	WR0E4	WR2E2	WR2E3	WR2E4
$t_{\rm WR}$ (10^3 yr)	0	0	0	2	2	2
$E_{\rm in}$ (10^{51} erg)	2	3	4	2	3	4
$R_{\rm fs}$(pc)	1.8	2.1	2.5	1.9	2.3	2.6
$R_{\rm rs}$(pc)	1.3	1.6	1.7	1.0	1.2	1.3

The observed locations[15] are $R_{\rm fs} = 2.5 \pm 0.2$ pc and $R_{\rm rs} = 1.6 \pm 0.2$ pc in Cas A. Therefore, only a model WR0E4 is fitted to the observations of both $R_{\rm fs}$ and $R_{\rm rs}$, which is consistent with the previous study.[21] As a consequence, we examine matter mixing due to the Rayleigh-Taylor instabilities for this model.

§4. Two dimensional hydrodynamical simulations and Rayleigh-Taylor instabilities

We performe two dimensional simulations of supernova explosion for the initial model WR0E4. Our region of calculation is divided into 1000 × 100 meshes in $r\theta$ plane. When the shock wave passes the boundary between C+O and He-rich layers at $t = 3.9$ s after the explosion, we specify purturbations in r-component of velocities as

$$\delta v_r = \epsilon v_r \cos(20\theta), \tag{4.1}$$

where we set $\epsilon = 0.1$. The Rayleigh-Taylor instability is judged from the criterion[22]

$$\nabla\rho \cdot \nabla P < 0. \tag{4.2}$$

This condition is satisfied in most regions of the boundary layers after the shock passes through.

During the propagation of the shock wave, we follow the abundance change using an α network code[23] which contains 13 nuclei from ^{4}He to ^{56}Ni. Furthermore, to evaluate the amount of radio actives nucleosynthesis is calculated in detail for tracer particles using the post process method with a large network code[24] of 464 nuclei. The produced amounts are found to be ^{44}Ti of 1.3×10^{-4} $M_\odot$ and ^{56}Ni of 0.123 $M_\odot$, whose values are consistent with the observed abundances.[25]

Figure 3 shows our results of simulations at $t = 330$ yr after the explosion. The left panel indicates the density contours, where the instability developes at $r \simeq 0.4$ and 1.6 pc. The former region is attributed to the boundary between original O- and Si-rich layers. The latter corresponds to the boundary between H- and He-rich layers. We note that in the deep O-rich layer, both Si and Fe are produced through the explosive O-burning. Most Fe are daughters of radioactive nuclei ^{56}Ni. As seen from the right panel, no mixing occurs between Si and Fe in our simulations.

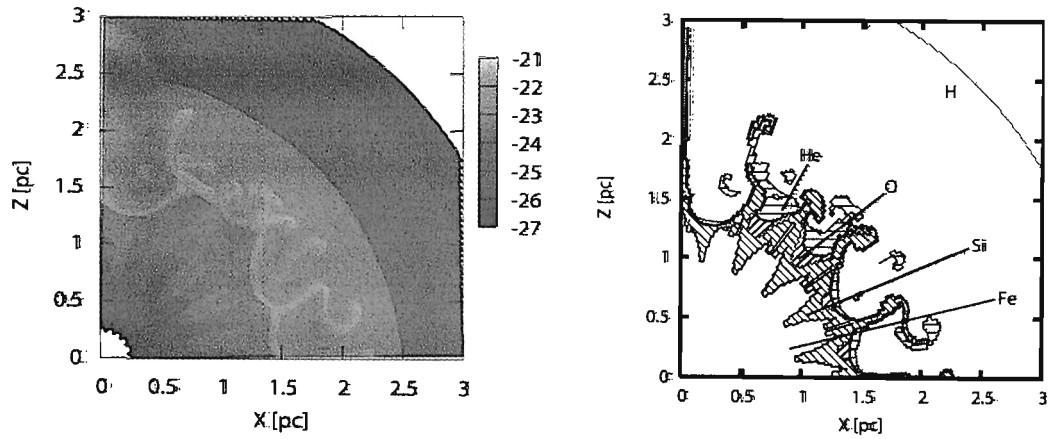

Fig. 3. Contours of the logarithm of density in units of g cm^{-3} (left panel) and the distribution of major elements (right panel) at $t = 330$ yr after the explosion. The dashed region of Si includes O, where the mass fraction of Si is larger than 5 % of that of O. The regions of He and O are occupied by almost these elements.

§5. Concluding remarks

In the present study, we have performed two dimensional simulations of supernova explosion and followed the abundance change during the propagation of the shock wave. We cannot find mixing of Si and Fe due to the Rayleigh-Taylor instability. However, after the shock passage instability criterion (4.2) always holds in a region of abundant Si and Fe. We would suggest possible issues for the mixing to be realized.

1) The resolution of calculations should be refined. We have divided the region into 1000×100 domains. It is difficult to follow both the shock wave outside the star and the Fe layers confined deep inside the star. Simulations of a core collapse supernova with higher resolution by using adaptive mesh refinement[26] may imply that our calculation is not enough to resolve the instabilities for matter mixing.

2) Other initial models should be checked. As seen from Fig. 3, the Si layer extends only to about 2 pc, which is inconsistent with the observations. This is ascribed to the distribution of the circumstellar medium. Figure 4 shows development of the forward shock, the reverse shock and the surface of Fe layer for models of WR0E4 (left panel) and WR2E4 (right panel). It is clear that there appears the difference in the way of shock propagation. In particular, the Fe layer catches up with the reverse shock at $t \simeq 2.5 \times 10^9$ s due to the collision of shocks and WR+RSG shell. Much larger scale mixing would be expected because the Rayleigh-Taylor instability is developed at the front of the reverse shock.[26] Our model WR0E4 could be inappropriate to induce the hydrodynamical instabilities in circumstellar medium. Therefore, shock propagation should be examined for different distributions of circumstellar medium.

3) Matter mixing could be originated from the mechanism of core collapse supernova. For example, standing accretion shock instability may induce the significant

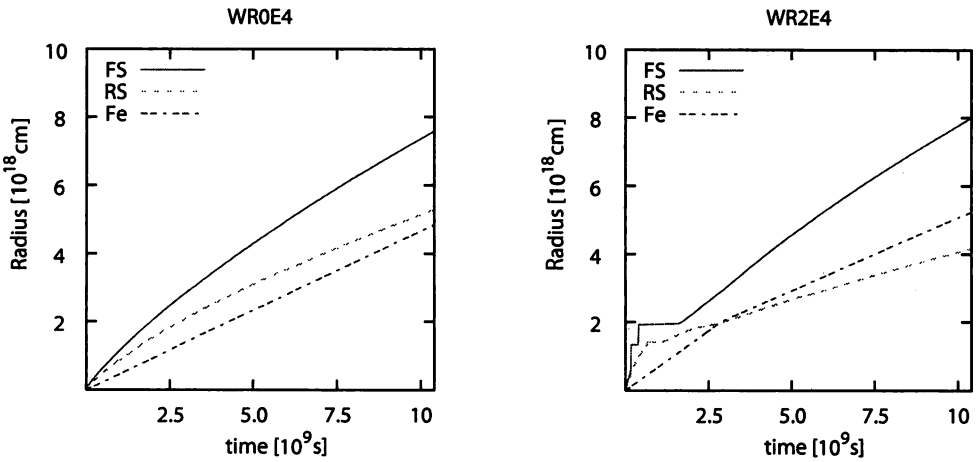

Fig. 4. Development of the forward shock (FS), the reverse shock (RS) and the surface of the Fe layer for models of WR0E4 (left panel) and WR2E4 (right panel). The Fe-surface overtakes RS at $T \simeq 2.5 \times 10^9$ s in WR2E4.

mixing between Si and Fe layers.

4) Large scale mixing could be realized through the three dimensional calculations as suggested by the observations. It is proposed that the Rayleigh-Taylor instability is more sufficiently developed in three dimensional calculations than two dimensional ones.[27)]

Acknowledgments

This work has been supported in part by a Grant-in-Aid for Scientific Research (19104006, 21540272) of the Ministry of Education, Culture, Sports, Science and Technology of Japan.

References

1) M. Ryle and G. Smith, Nature **162** (1948), 462.
2) M. Anerson et al., Astrophys. J. **373** (1991), 146.
J. W. Keohane, L. Rudnick and M. C. Anderson, Astrophys. J. **466** (1996), 1309.
3) O. Krause et al., Science **308** (2005), 604.
J. A. Ennis et al., Astrophys. J. **652** (2006), 376.
4) R. A. Fesen and K. S. Gunderson, Astrophys. J. **652** (1996), 376.
J. A. Morse et al., Astrophys. J. **614** (2004), 727.
5) R. Willingele et al., Astron. Astrophys. **398** (2003), 1021.
U. Hwang and J. M. Laming, Astrophys. J. **597** (2003), 362.
6) R. A. Fesen, G. G. Pavlov and D. Sanmal, Astrophys. J. **645** (2006), 283.
7) J. E. Reed, J. J. Hester, A. C. Fabian and P. E. Winkler, Astrophys. J. **440** (1995), 706.
8) R. A. Fesen, R. H. Becker and W. P. Blair, Astrophys. J. **313** (1987), 378.
S. E. Woosley, N. Langer and T. A. Weaver, Astrophys. J. **411** (1993), 823.
9) O. Krause et al., Science **320** (2008), 1195.
10) J. Vink, New Astron. Rev. **48** (2004), 61.
U. Hwang et al. Astrophys. J. **615** (2004), L117.
J. P. Hughes et al., Astrophys. J. **528** (2000), L109.
11) I. Hachisu, T. Matsuda, K. Nomoto and T. Shigeyama, Astrophys. J. **358** (1990), L57.
12) B. Pérez-Rendón, G. García-Segura and N. Langer, Astron. Astrophys. **506** (2009), 1249.

11) I. Hachisu, T. Matsuda, K. Nomoto and T. Shigeyama, Astrophys. J. **358** (1990), L57.
12) B. Pérez-Rendón, G. García-Segura and N. Langer, Astron. Astrophys. **506** (2009), 1249.
13) J. M. Blondin, A. Mezzacappa and C. Demarino, Astrophys. J. **584** (2003), 971.
14) S. Nagataki, T. M. Shimizu and K. Sato, Astrophys. J. **495** (1998), 413.
15) E. V. Gotthelf et al., Astrophys. J. **552** (2001), L39.
16) T. Nozawa et al., Astrophys. J. **713** (2009) 356.
17) R. Hirschi, G. Meynet and A. Maeder, Astron. Astrophys. **425** (2004), 649.
18) T. Nugis and H. J. G. L. M. Lamers, Astron. Astrophys. **360** (2000), 227.
19) K. M. Schure et al., Astrophys. J. **686** (2008), 399.
20) M. Hashimoto, Prog. Theor. Phys. **94** (1995), 663.
21) B. van Veelen et al., Astron. Astrophys. **503** (2009), 495.
22) H. Takabe, Jap. Soc. Plasma Sci. Nuc. Fusion Res. **69** (1993), 1285.
23) E. Müller, Astron. Astrophys. **162** (1986), 103.
24) M. Ono, M. Hashimoto, S. Fujimoto, K. Kotake and S. Yamada, Prog. Theor. Phys. **122** (2009), 755.
25) J. Vink et al., Astrophys. J. **560** (2001), L79.
P. A. Young et al., Astrophys. J. **640** (2006), 891.
26) K. Kifonidis et al., Astron. Astrophys. **453** (2006), 661.
27) A. Noro, T. Ohta, T. Ogawa, K. Yamashita and S. Miyaji, HPCS (2002), 9.